XI International Conference on Computational Plasticity. Fundamentals and Applications
COMPLAS XI
E. Oñate, D.R.J. Owen, D. Peric and B. Suárez (Eds)

ACCELERATED ENERGY-MINIMIZATION IN THE QUASICONTINUUM METHOD WITH APPLICATION TO NANOPILLAR COMPRESSION

B. EIDEL*, A. STUKOWSKI† AND J. SCHRÖDER*

*Institute for Mechanics, Faculty of Engineering Sciences
University of Duisburg-Essen
Universitätsstr. 15, 45141 Essen, Germany
e-mail: bernhard.eidel@uni-due.de, www.uni-due.de/mechanika/

†Lawrence Livermore National Laboratory (LLNL)
7000 East Avenue, Livermore, CA 94550, USA
e-mail: stukowski1@llnl.gov, https://www.llnl.gov/

Key words: Multiscale Materials Modeling, Atomic-to-Continuum Coupling, Energy-Minimization, Finite Element Method, Quasicontinuum

Abstract. The focus of this contribution is on a novel, improved technique for energy minimization in atomic simulations and its adaption to a variationally consistent formulation of the quasicontinuum (QC) method. The optimization algorithm called FIRE for Fast Inertial Relaxation Engine can be understood as a modification of the Steepest Descent (SD) method, which improves SD by accelerating the system in the direction of the force, making the minimization more aggressive. The performance of FIRE is assessed in the example of nanopillar compression with respect to efficiency and stability against competitive optimization methods.

1 MODELING

1.1 Fully nonlocal QC method based on energy calculation in clusters.

The main conceptual ingredients of the fully nonlocal QC-method which drastically reduce the computational burden of fully atomistic models are visualized in Fig. 1. Firstly, it is a finite element discretization ('coarse-graining') reducing the number of degrees of freedom in the crystal. Secondly, and even more important for reducing the computational costs, it is the calculation of atomic energies $E_{\boldsymbol{k}}$ at lattice sites $\boldsymbol{k}$ in spherical sampling clusters $\mathscr{C}_{\boldsymbol{i}}$ of radius R_c defined as $\mathscr{C}_{\boldsymbol{i}} = \{\boldsymbol{k} : |\boldsymbol{X}_{\boldsymbol{k}} - \boldsymbol{X}_{\boldsymbol{i}}| \leq R_c(\boldsymbol{i})\}$ instead of in the entire crystal. The energy of each cluster is multiplied with a weighting factor $n_{\boldsymbol{i}}$ accounting for the energy contributions of atoms outside the cluster. The summation over all mesh

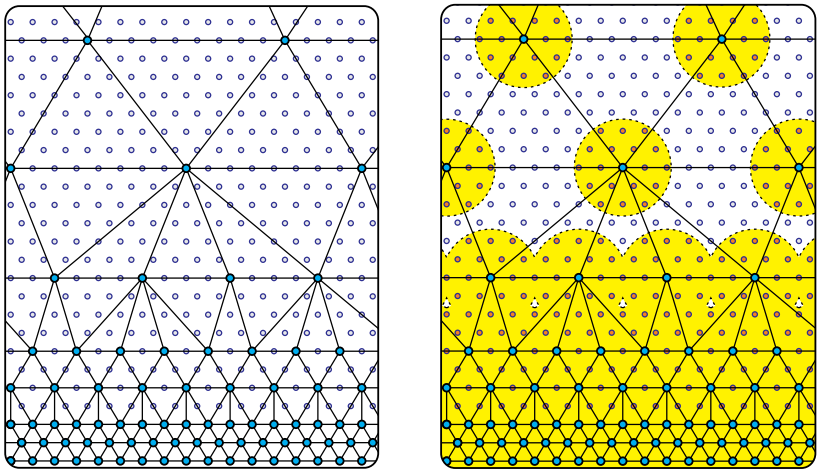

Figure 1: Approximations in the cluster-based QC method: (Left) Finite element discretization of the crystal where atoms in the interior of elements smoothly follow the deformation of the representative atoms (mesh nodes) by linear interpolation. (Right) Energy sampling in spherical clusters.

nodes $\boldsymbol{i} \in \mathscr{L}_h$ and therefore over all clusters yields the QC-approximation of the total energy

$$E^{\mathrm{QC}} = \sum_{\boldsymbol{i}\in\mathscr{L}_h} n_{\boldsymbol{i}} \sum_{\boldsymbol{k}\in\mathscr{C}_{\boldsymbol{i}}} E_{\boldsymbol{k}}\,. \tag{1}$$

The atomic energies $E_{\boldsymbol{k}}$ are calculated using pair functionals of the Embedded Atom Method (EAM). Note, that the cluster radius R_c is a purely numerical parameter controlling the accuracy of the cluster summation rule, whereas the cut-off radius is a physical parameter and cannot be arbitrarily chosen. The weighting factors $n_{\boldsymbol{i}}$ are calculated such that the sum of the shape function values in the clusters multiplied with the weighting factors equals the sum of the shape function values at all lattice sites in the crystal, it reads

$$\sum_{\boldsymbol{i}\in\mathscr{L}_h} n_{\boldsymbol{i}} \sum_{\boldsymbol{k}\in\mathscr{C}_{\boldsymbol{i}}} \varphi_{\boldsymbol{j}}(\boldsymbol{X}_{\boldsymbol{k}}) = \sum_{\boldsymbol{k}\in\mathscr{L}} \varphi_{\boldsymbol{j}}(\boldsymbol{X}_{\boldsymbol{k}}) \qquad \forall \quad \boldsymbol{j} \in \mathscr{L}_h\,. \tag{2}$$

Stable equilibrium configurations of the crystal are minimizers of the total energy and correspond to configurations for which the resultant force at every finite element node $\boldsymbol{a}$ is zero, hence

$$\min_{\{\boldsymbol{x}_{\boldsymbol{a}}\}} E^{\mathrm{QC}} \quad \Longrightarrow \quad \boldsymbol{f}_{\boldsymbol{a}}^{\mathrm{QC}} = -\frac{\partial E^{\mathrm{QC}}}{\partial \boldsymbol{x}_{\boldsymbol{a}}} = \boldsymbol{0} \qquad \forall \quad \boldsymbol{a} \in \mathscr{L}_h\,. \tag{3}$$

For more details about the cluster-based QC method, we refer to [7] and [4], a comparison with the QC method based on Cauchy-Born elasticity can be found e.g. in [5] and [6].

1.2 Energy minimization based on acceleration and inertia

Energy minimization in atomic simulations at zero temperature is used to find the (inherent) equilibrium structure of a solid without the "noise" of thermal vibrations. When the equilibrium structure is searched at finite temperature, an established technique is to carry out molecular dynamics (MD) calculations, but then, to remove continuously kinetic energy from the system, a process called numerical "quenching". In [1] a simple MD scheme for structural relaxation was proposed which belongs to this class of minimizers. The algorithm dubbed FIRE for *Fast Inertial Relaxation Engine* (FIRE) crucially relies on inertia as its precursor Quick-Min (QM) does, see [2], but makes effective improvements. The strategy to descent to a minimum of the total energy is to follow an equation of motion given by

$$\dot{\boldsymbol{v}}(t) = 1/m\, \boldsymbol{F}(t) - \gamma(t)|\boldsymbol{v}(t)| \left[\hat{\boldsymbol{v}}(t) - \hat{\boldsymbol{F}}(t)\right], \tag{4}$$

with mass m, velocity $\boldsymbol{v} = \dot{\boldsymbol{x}}$, force $\boldsymbol{F} = -\nabla E^{\mathrm{QC}}(\boldsymbol{x})$, and where the hat denotes a unit vector. Hence, the strategy is to accelerate in a direction that is "steeper" than the current direction of motion via the function $\gamma(t)$, if the power $P(t) = \boldsymbol{F}(t) \cdot \boldsymbol{v}(t)$ is positive. To avoid uphill motion the algorithm stops as soon as the power becomes negative. The parameter $\gamma(t)$ must be chosen appropriately but should not be too large, because the current velocities carry information about the reasonable 'average' descent direction and energy scale, see [1]. The numerical treatment of the algorithm is based on an MD integrator like the Velocity Verlet algorithm providing the propagation of the trajectories due to conservative forces. The MD trajectories are continuously readjusted by a mixing rule of the velocities according to

$$\boldsymbol{v} \to (1-\alpha)\boldsymbol{v} + \alpha \hat{\boldsymbol{F}}|\boldsymbol{v}| \tag{5}$$

which follows from an Euler-step of the second term on the right in eq. (4) with time step size Δt and $\alpha = \gamma \Delta t$. The propagation rules for the FIRE algorithm can be summarized as follows (initialization: set values for Δt, $\alpha = \alpha_{\mathrm{start}}$, the global vectors $\boldsymbol{x}$ and set $\boldsymbol{v} = \boldsymbol{0}$):

1. MD integrator: calculate $\boldsymbol{x}$, $\boldsymbol{F} = -\nabla E^{\mathrm{QC}}(\boldsymbol{x})$ and $\boldsymbol{v}$ using any common MD integrator (here: Velocity Verlet); check for convergence.
2. calculate force power $P = \boldsymbol{F} \cdot \boldsymbol{v}$.
3. set $\boldsymbol{v} \to (1-\alpha)\boldsymbol{v} + \alpha|\boldsymbol{v}|\hat{\boldsymbol{F}}$.
4. if $P > 0$ and the number of steps since P was negative is larger than N_{min}, increase the time step $\Delta t \to \min(\Delta t f_{\mathrm{inc}}, \Delta t_{\mathrm{max}})$ and decrease $\alpha \to \alpha f_{\alpha}$.
5. if $P \leq 0$, decrease time step $\Delta t \to \Delta t f_{\mathrm{dec}}$, freeze the system $\boldsymbol{v} \to \boldsymbol{0}$, and set α back to α_{start}.
6. Return to MD integrator.

The FIRE-parameters used in the present work are set to $N_{\min} = 5$, $\alpha_{\text{start}} = 0.1$, $f_{\text{inc}} = 1.1$, $f_{\text{dec}} = 0.5$ and $f_\alpha = 0.99$.

Remark.
The differences of FIRE compared with its precursor QM are twofold. Both algorithms take dynamical steps starting in the direction of the steepest descent. Furthermore they both reset the velocity if the force and velocity are in opposite directions. The first difference is, however, that FIRE employs variable time step sizes. The second difference is that QM projects the velocity onto the force vector according to

$$\boldsymbol{v} \to (\boldsymbol{v} \cdot \hat{\boldsymbol{F}})\hat{\boldsymbol{F}} \tag{6}$$

whereas FIRE only projects a component of the velocity in the force direction, while maintaining momentum in other directions, see eq.(5), which avoids to adjust the direction of descent too hastily.

2 EXAMPLE: COMPRESSION OF A NANOPILLAR

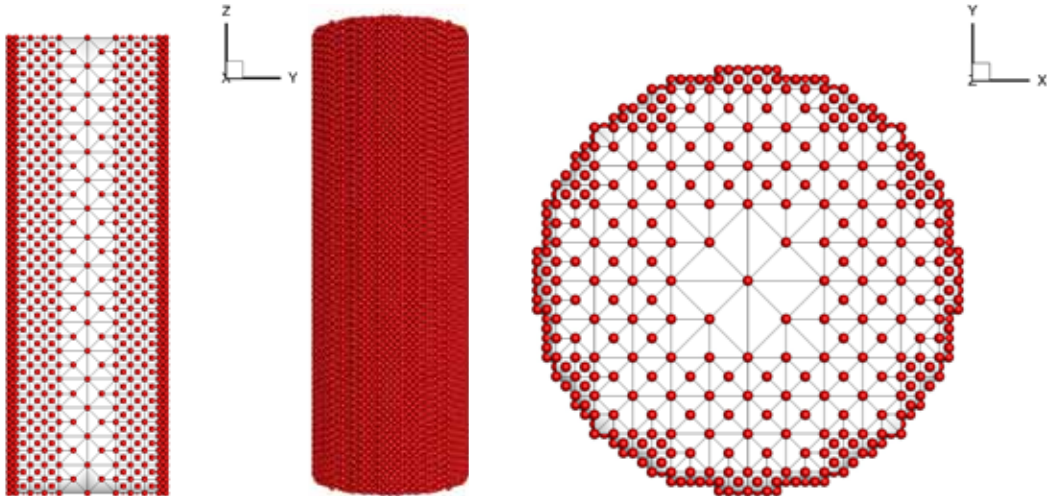

Figure 2: Nanopillar compression, (left) lateral cross sectional view of the discretization, (center) outer face, (right) cross sectional view of discretization reveals the approximation of the circle by a polygon due to the small size of the fcc pillar.

The single-crystalline, fcc nanopillar made of aluminum is of cylindrical shape and exhibits height $H = 64\,a_0$, diameter $D = 16\,a_0$ with lattice constant $a_0 = 4.032$ Å. Crystallographic $< 001 >$-axes align with cartesian X-, Y- and Z-axes. The pillar is supported at the bottom in z-direction and all faces are free surfaces. After initial relaxation of the crystal without the presence of external forces, the top surface is loaded by a compressive force, which is mediated by displacement control in z-direction. For a proper geometry description the curved surface is in full atomic resolution, whereas the interior of the pillar

is initially coarse-grained by finite elements. The cluster radius in the simulations is set to $R_c = a_0/\sqrt{2}$, for the energy calculation an EAM-potential for aluminum is used.

The novel FIRE minimizer is tested against the performance of the Steepest Descent (SD) method, a nonlinear version of the Conjugate Gradient (CG) method and the Limited-memory Broyden-Fletcher-Goldfarb-Shanno (L-BFGS) algorithm. The total deformation range can be decomposed into three distinct ranges.

(I) For *surface relaxations* the energy landscape is typically rather flat, the process of energy-minimization using conventional optimization algorithms tends to get trapped in shallow holes representing local energy minimizers as indicated by residuals toggling up and down but cannot go below an accuracy threshold. FIRE in contrast, by virtue of its inertia can pass these local minima and can achieve virtually arbitrary accuracy. For the surface relaxation in the present example the performance of FIRE is in between L-BFGS and the CG method, the convergence of SD is very slow, see the top diagram in Fig. 3.

(II) The range of *elastic compression* is very ample and extends to a maximum compressive strain of 7.7%. The reason is that the pillar exhibits no initial dislocations which can serve as carriers of plastic deformation. Therefore, the present compression simulation probes the strength of the material rather than giving an example of classical, dislocation-mediated plasticity on the nanoscale. The diagram in the center of Fig. 3 belongs to a single loading step which is representative for the performance of the minimization algorithms in the entire elastic deformation range. FIRE performs better than the other optimizers and is even considerably faster than L-BFGS.

(III) At the point of *material instability*, where strain localizes in a crystallographic slip band coinciding with a {111} plane, CG and SD diverge, whereas L-BFGS and FIRE can pass the point of bifurcation. Here, FIRE is faster than L-BFGS, see the bottom in Fig. 3.

2.1 A note on the mechanics of nano-/micropillars

The mechanics of small-sized (diameter D in the range of approximately 100 nm – 2 μm), single-crystalline pillars has attracted considerable interest in recent years. The reason is that for these pillars subject to compression a size-dependence of the flow stress in the sense of "smaller is stronger" has been measured, which was first reported in [3]. This behavior seems to be at odds with an earlier understanding, according to which size-dependence requires structural obstacles to dislocation motion like grain-boundaries or other interfaces (cf. Hall-Petch relationship). A single-crystalline specimen with a deformation state assumed to be quasi-homogeneous in contrast, was not expected to exhibit that size-dependence.

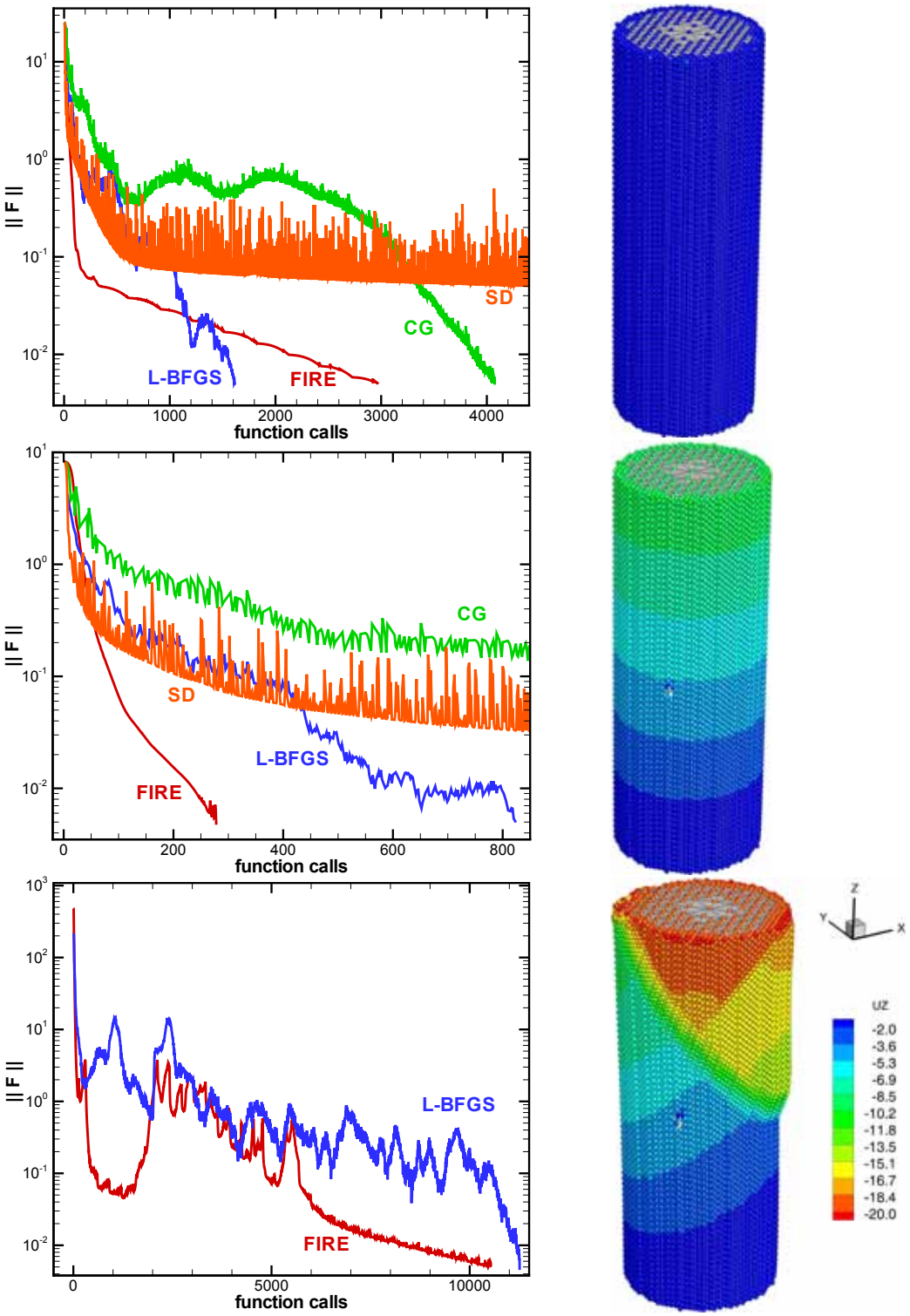

Figure 3: Convergence diagrams for different optimizers at characteristic deformation stages of the compressed nanopillar (left), contour plots for displacement component u_z [Å] (right).

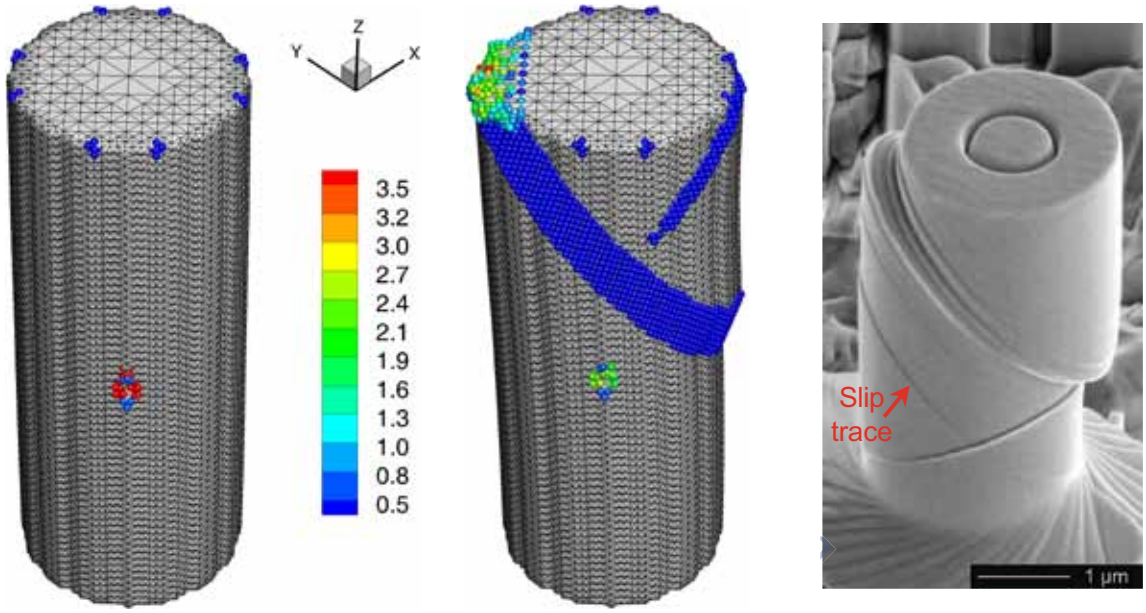

Figure 4: Compression of single-crystalline fcc nano-/micropillar. Deformed pillar right before (Left) and right after bifurcation (centre) with contour plots for $II(\mathrm{dev}\boldsymbol{E}) > 0.3$ in QC-simulation for Al and (right) in the experiment of a Ni-micropillar, picture from [3].

Note, that for the present simulations one atom has been removed from the middle of the pillar's surface in order to attract stress at that local defect and thereby to trigger localization. This can be best seen in the left of Fig. 4, where atoms are displayed that exhibit a value for the second invariant of the Green-Lagrangian strain tensor $II(\mathrm{dev}\boldsymbol{E}) > 0.3$. Note that right before localization the largest deviatoric strain is observed at the site where the atom is removed. Nevertheless, localization starts from the intersecting surfaces at the loaded top, Fig. 4 (center), which indicates that this geometrical defect is stronger than the artificially introduced surface defect. Furthermore the contour plot of $II(\mathrm{dev}\boldsymbol{E})$ in Fig. 4 reveals that right after the first microband has formed, a second slip system is activated.

3 CONCLUSION

Summarizing, in its modified formulation within the quasicontinuum method, FIRE is competitive with, in some cases superior to well-established efficient minimization algorithms like L-BFGS. Beyond its superior behavior with respect to *efficiency* and *stability* FIRE is easy to implement and can be operated intuitively. These benefits and promising results suggest to use FIRE in various other models, especially when stability issues are a major concern.

REFERENCES

[1] Bitzek, E., Koskinen, P., Gähler, F., Moseler, M., and Gumbsch, P. Structural relaxation made simple. *Phys. Rev. Lett.* (2006) **97**:170201(4).

[2] Della Valle, R.G. and Jonsson, H.C. Molecular dynamics simulation of silica liquid and glass. *J. Chem. Phys.* (1992) **97(4)**:2682–2689.

[3] Dimiduk, D.M., Uchic, M.D., and Parthasarathy, T.A. Size-affected single-slip behavior of pure nickel microcrystals. *Acta Mater.* (2005) **53**:4065–4077.

[4] Eidel, B. and Stukowski, A. A variational formulation of the quasicontinuum method based on energy sampling in clusters. *J. Mech. Phys. Solids* (2009) **57**:87–108.

[5] Eidel, B. Coupling atomistic accuracy with continuum effectivity for predictive simulations in materials research - the Quasicontinuum Method. *Int. J. Mat. Res.* (2009) **100**:1503–1512.

[6] Eidel, B., Hartmaier, A., and Gumbsch, P. Atomistic Simulation Methods and their Application on Fracture, In: *Multiscale Modelling of Plasticity and Fracture by Means of Dislocation Mechanics*. CISM International Centre for Mechanical Sciences, Courses and Lectures, Vol. 522, 1–58, Springer, (2010).

[7] Knap, J. and Ortiz, M. An analysis of the quasicontinuum method. *J. Mech. Phys. Solids* (2001) **49**:1899–1923.